Numerical Algebraic Geometry and Differential Equations

Wenrui Hao* Bei Hu† Andrew J. Sommese‡

September 20, 2012

Abstract

In this paper we review applications of numerical algebraic geometry to differential equations. The techniques we address are direct solution, bootstrapping by filtering, and continuation and bifurcation. We review differential equations systems with multiple solutions and bifurcations.
Keywords. Numerical algebraic geometry, polynomial system, algebraic sets, witness sets, projections, membership test, numerical irreducible decomposition
AMS Subject Classification. 65H10, 68W30

Introduction

Most systems of nonlinear differential equations are not solvable in an explicit form, nor is the structure of the solutions; the number of solutions; or even the existence of a single solution with given boundary conditions. For these reasons, users of mathematics are forced to resort to numerical methods, though for nonlinear systems, traditional numerical methods usually do not suffice.

*Department of Applied and Computational Mathematics and Statistics, University of Notre Dame, Notre Dame, IN 46556 (whao@nd.edu, www.nd.edu/∼whao). This author was supported by the Duncan Chair of the University of Notre Dame.

†Department of Applied and Computational Mathematics and Statistics, University of Notre Dame, Notre Dame, IN 46556 (b1hu@nd.edu, www.nd.edu/∼b1hu).

‡Department of Applied and Computational Mathematics and Statistics, University of Notre Dame, Notre Dame, IN 46556 (sommese@nd.edu, www.nd.edu/∼sommese). This author was supported by the Duncan Chair of the University of Notre Dame.

In recent years, remarkable progress has been made in the development and implementation of efficient algorithms to numerically solve and manipulate solutions of systems of polynomial equations. For some background on this field, called Numerical Algebraic Geometry, see [30, 35, 38]. Many systems, when discretized, lead to systems of polynomials. In the last few years, methods of numerical algebraic geometry have begun to be used to investigate and solve systems of discretized nonlinear differential equations.

In this article, we will give an overview of the new approach and some of the systems that have been successfully investigated and solved by these new methods. The new approach has been based on combinations of three techniques:

1. direct solution of the polynomial systems that arise [18] and[28, §9.4];

2. bootstrap methods [1, 23] to solve large systems by building up to them from smaller systems; and

3. construction of new branches of solutions out of existing branches of solutions by computation of bifurcation points and continuation of solutions along the distinct branches coming out of the the bifurcation points [19, 20, 21, 22, 24, 25, 26].

1 Direct solution

In this section we give some nontrivial examples of systems, where direct solution has been used. The combination of efficient new parallel algorithms; increasingly inexpensive clusters; and the polynomial solver Bertini [4] has led to the ability to solve discretizations with over forty polynomials in forty variables.

Given the exponential growth of the number of numerical solutions of the polynomial systems that arise through discretization as the number of nodes increase, the direct methods by themselves are hopeless. Nevertheless brute-force methods do allow significant information to be computed for a number of nontrivial systems, and combined with the bootstrap approaches explained in §2 and §3 allow us to compute many solutions for several nontrivial discretizations with thousands of variables.

1.1 A Lotka-Volterra population model with diffusion

As a first example, consider the following Lotka-Volterra population model with diffusion [32, 37] on the first quadrant square $\mathcal{R} := [0,1] \times [0,1] \subset \mathbb{R}^2$:

$$\begin{aligned} -\Delta u &= u(1-v) && (1)\\ -\Delta v &= -v(1-u), && (2) \end{aligned}$$

where Δ is the Laplacian and u and v are functions defined on $\mathcal{R}$, which are taken some non-zero boundary condition. For example,

$$u = \begin{cases} 0 & \text{if } x = 0 \\ 1 & \text{if } x = 1 \\ x & \text{if } y = 0, \\ \sin(x)/\sin(1) & \text{if } y = 1, \end{cases} \quad \text{and } v = \begin{cases} 1 & \text{if } x = 0, \\ 0 & \text{if } x = 1, \\ 1-x & \text{if } y = 0, \\ \sin(1-x)/\sin(1) & \text{if } y = 1. \end{cases}$$

Discretizing using central differences with the gridpoints

$$(x_i, y_j) = \left(\frac{i}{5}, \frac{j}{n+1}\right) \quad \text{for } 0 \le j \le 5; 0 \le i \le n$$

for some positive integer n, we have the polynomial system with $8n$ equations

$$\begin{aligned} \frac{u_{i+1,j} - 2u_{i,j} + u_{i-1,j}}{25} + \frac{u_{i,j+1} - 2u_{i,j} + u_{i,j-1}}{(n+1)^2} + \frac{u_{i,j}(1-v_{i,j})}{25(n+1)^2} &= 0 && (3)\\ \frac{v_{i+1,j} - 2v_{i,j} + v_{i-1,j}}{25} + \frac{v_{i,j+1} - 2v_{i,j} + v_{i,j-1}}{(n+1)^2} + \frac{v_{i,j}(u_{i,j}-1)}{25(n+1)^2} &= 0 && (4) \end{aligned}$$

with variables $\{u_{i,j}, v_{i,j} \mid 1 \le i \le n, 1 \le j \le 4\}$ and constants

$$u_{0,j} = v_{n+1,j} = 0,\ u_{n+1,j} = v_{0,j} = 1,$$

$$u_{i,0} = i/5,\ u_{i,5} = \frac{\sin(i/5)}{\sin(1)},\ v_{i,0} = 1 - i/5,\ v_{i,5} = \frac{\sin(1-i/5)}{\sin(1)}.$$

This system, which was investigated numerically by Hauenstein, Hu, and Sommese, is a good example of the growth of solutions of the discretization as the gridsize grows. In [28, §9.4] a related (and practically equivalent) polynomial system was used as one of the test examples for the polynomial-system solving method called regeneration. All equations are quadratic with total degree 2^{8n}, though the system has only 2^{4n} solutions. Bertini took 7.36 minutes when $n = 4$ and 3.81 hours when $n = 5$ when run in parallel on 64 cores (8 nodes each with two 2.33 GHz

quad-core Xeon 5410s). Though this grid is fine enough to get some useful information, the computing times make clear that (even with more cores), the brute force approach is limited. The main numerical polynomial system solvers Bertini [4], HOM4PS-2.0 [29], and PHC [29] were compared on the system of [28, §9.4]: only Bertini could deal with the larger systems.

Nevertheless direct computation can be very useful in some cases. The patterning model of Zhang, Lander, and Nie[39] leads to a system of four nonlinear ordinary differential equations of the form (5). We refer to [18], where this system of differential equations is written out in detail and explained (there are biologically relevant constants). In non-dimensionalized form the system was shown to be [18, Eq. 3.6]

$$\begin{cases} \dfrac{\partial A}{\partial T} = \dfrac{\partial^2 A}{\partial X^2} + H_1(A, B, C, S, T); \\ \dfrac{\partial B}{\partial T} = H_2(A, B); \\ \dfrac{\partial C}{\partial T} = \dfrac{\partial^2 C}{\partial X^2} + H_3(A, S, C); \\ \dfrac{\partial S}{\partial T} = \dfrac{\partial^2 S}{\partial X^2} + H_4(A, B, C, T), \end{cases} \tag{5}$$

where $0 \leq X \leq 1$ and the H_i are some specific (but involved) nonlinear functions.. Using an interval with eleven points, the associated polynomial system was solved using Bertini. This took about eleven hours using 200 cores (25 nodes each with two 2.33 GHz quad-core Xeon 5410s). The associated polynomial system had 384,064 complex solutions of which 17,974 were real. Of these, only seven satisfied the physically necessary condition that they are positive. Three of the seven were shown to be stable. Many of the seven solutions were new and would have been very difficult to compute by standard methods such as time-marching.

2 Bootstrapping by filtering

Given the systems in §1, we see that for polynomial system methods to be of broad use, we need to be able to cut the exponential growth of solutions as the number of grid points grows. One way to do this [1, 2, 3] is *filtering*. To explain this approach consider the example following ordinary differential equation on $[0, 1]$, which is know to have infinitely many solutions [1, §3.3]:

$$y'' = -y^3. \qquad y(0) = y(1) = 0. \tag{6}$$

Discretized we have the polynomial systems F_N indexed by integers $N \geq 1$

$$F_N(y) := \begin{bmatrix} \frac{y_2 - 2y_1}{h^2} + y_1^3 \\ \frac{y_3 - 2y_2 + y_1}{h^2} + y_2^3 \\ \vdots \\ \frac{y_N - 2y_{N-1} + y_{N-2}}{h^2} + y_{N-1}^3 \\ \frac{-2y_N + y_{N-1}}{h^2} + y_N^3 \end{bmatrix} = 0 \tag{7}$$

for $N = 1, 2, 3, \ldots$, where $h = 1/(N+1)$, $y_0 = y_{N+1} = 0$, and for $1 \leq i \leq N+1$, y_i is the approximate value of a given possible solution at $x_i = i/(N+1)$. Here we have presented the system as if $N \geq 4$ so that the pattern is clear.

Of course, we cannot numerically compute all solutions since there are an infinite number, but we would like to compute a good selection of solutions for increasing N. Only a small fraction (see [1]) of the solutions for any N are real.

The idea of filtering is start with some set $\mathcal{U}_N$ of isolated solutions of $F_N(y) = 0$. To get to solutions of $F_{N+1}(y) = 0$

1. use some filtering condition (for example, having small imaginary parts) to discard solutions, leaving a set $\mathcal{S}_N$ of solutions of $F_N(y) = 0$;

2. construct a polynomial system in $y_1, \ldots, y_{N+1}$ of the form

$$\Phi(y_1, \ldots, y_N, y_{N+1}) = \begin{bmatrix} F_N(y_1, \ldots, y_N) \\ g(y_1, \ldots, y_N, y_{N+1}) \end{bmatrix} = 0;$$

3. compute the solutions $\mathcal{I}_{N+1}$ of $\Phi(y_1, \ldots, y_{N+1}) = 0$ with $(y_1, \ldots, y_N) = y^*$ for some $y^* \in \mathcal{S}_N$;

4. construct a homotopy $H(y_1, \ldots, y_{N+1}, t) = 0$ with $t \in [0, 1]$; $H(y, 1) = \Phi(y)$; and $H(y, 0) = F_{N+1}(y)$;

5. use $H(y, t)$ to continue the solutions $\mathcal{I}_{N+1}$ to solutions $\mathcal{U}_{N+1}$ of $F_{N+1} = 0$.

This process will typically start with all solutions of $F_{N_0} = 0$ for a small integer N_0. Clearly there are a lot of choices. Moreover we might add more nodes at each step.

3 Bootstrapping by Domain Decomposition

Though filtering works well with ordinary differential equations, it, by itself, has not worked well with systems of nonlinear partial differential equations. In [23],

we introduce a new bootstrapping method to use domain decomposition to guide us in building up to a polynomial system (arising by discretization) from simpler polynomial systems (arising from coarser discretizations and discretizations over smaller regions). This new method combines well with filtering to yield many unknown solutions of interesting systems. In [23, §5], this method is used to yield many highly nontrivial solutions of complicated tumor growth models of the sort discussed in §4. Here we just give a simple illustrative ordinary differential equation example.

Consider the system

$$u_{xx} = f(u) \text{ on } (0,1); \qquad u(0) = u_0, \quad u(1) = u_1 \tag{8}$$

for some polynomial $f(u)$: in the article [23], a number of different $f(u)$ are used in examples.

Our goal is to first solve Eq. 8 on the interval $[0,1]$ with NM grid points where N and M are two small integers. To do this

1. we first solve Eq. 8 for the gridpoints at $x_i = iH$, where $i = 0, \ldots, N$ and $H = 1/N$ and use some filter to discard unreasonable solutions;

2. next we solve
$$u_{xx} = f(u)$$
with M gridpoints on each of the intervals $[x_i, x_{i+1}]$ with boundary conditions given by using the solutions in step 1); and

3. we use a homotopy to continue the solutions of step 2) into solutions of a discretization of Eq. 8 with NM gridpoints.

We first solve

$$C_N(u_1, \ldots, u_{N-1}) = \begin{bmatrix} u_2 - 2u_1 + u_0 & - & H^2 f(u_1) \\ & \vdots & \\ u_N - 2u_{N-1} + u_{N-2} & - & H^2 f(u_{N-1}) \end{bmatrix} = 0. \tag{9}$$

Let $x_{i,j} = x_i + jh$ where $h = 1/M$ and $j = 0, \ldots, M$ Note that $x_{i,0} = x_i$ and $x_{i,M} = x_{i+1}$. We wish to compute an approximation $u_{i,j}$ to a solution $u(x_{i,j})$ of Eq. 8 using the discretization with $NM - 1$ variables and equations

$$\mathcal{F}_{NM}(U) = \begin{bmatrix} u_{0,2} - 2u_{0,1} + u_{0,0} - (hH)^2 f(u_{0,1}) \\ \vdots \\ u_{N-1,M} - 2u_{N-1,M-1} + u_{N-1,M-2} - (hH)^2 f(u_{N-1,M-1}) \end{bmatrix} = 0 \tag{10}$$

where we let U denote $(u_{0,1}, \ldots, u_{0,M-1}, u_{1,0} \ldots, u_{1,0}, \ldots, u_{N-1,0}, \ldots, u_{N-1,M-1})$ and make the convention that the variables $u_{i,N}$ and $u_{i+1,0}$ are the same for $i = 0, \ldots N-1$, $u_{N-1,M} = u(1)$, and $u_{0,0} = u(0)$. For each solution $(u_0, \ldots, u_N)$ of Eq. 9, compute approximate solutions to the systems

$$u_{xx} = f(u) \text{ on } [x_i, x_{i+1}]; \quad u(x_i) = u_i, \quad u(x_{i+1}) = u_{i+1}$$

using the systems

$$SS_{i,M}(u_{i,0}, u_{i,1}, \ldots, u_{i,M-1}, u_{i,M}) = \begin{bmatrix} u_{i,2} - 2u_{i,1} + u_{i,0} & - & h^2 f(u_{i,1}) \\ & \vdots & \\ u_{i,M} - 2u_{i,M-1} + u_{i,M-2} & - & h^2 f(u_{M-1}) \end{bmatrix} = 0 \tag{11}$$

for $i = 0, \ldots, N-1$ with $u_{0,0} = u_0$ and $u_{N-1,M} = u_1$.

We thus have a set of solutions of the composite system

$$P_N(U) = \begin{bmatrix} C_N(u_{0,M}, u_{1,M}, \ldots, u_{N-1,M}) \\ SS_{0,M}(u_{0,0}, u_{0,1}, \ldots, u_{0,M}) \\ \vdots \\ SS_{N-1,M}(u_{N-1,0}, \ldots, u_{N-1,M}) \end{bmatrix} = 0. \tag{12}$$

Next we track these solutions as t goes from 1 to 0 using a homotopy such as

$$H(U,t) = (1-t)\mathcal{F}_{NM}(u_{0,1}, \ldots, u_{N-1,M-1}) + t \begin{bmatrix} C_N(u_1, \ldots, u_{N-1}) \\ SS_{0,M}(u_{0,0}, \ldots, u_{0,M}) \\ \vdots \\ SS_{N-1,M}(u_{N-1,0}, \ldots, u_{N-1,M}) \end{bmatrix}.$$

Finally filtering the solutions of $H(U, 0)$.

4 Continuation and Bifurcation

In this section we only discuss the free boundary problems arising in tumor growth [19, 20, 21, 22, 23] that we have investigated using the new methods. These methods apply to other biological models [24, 25].

The free boundary problems are of the type

$$V_n(x,t) = F[\mathcal{O}_(t), \vec{u}(x,t), \lambda], \quad x \in \Gamma(t), \quad t > 0, \tag{13}$$

where $\vec{u}(x,t)$ is typically a solution of a system of partial differential equations in the domain $x \in \mathcal{O}_(t), t > 0$ which is changing over time, $V_n(x,t)$ $(x \in \Gamma(t))$ is the

normal velocity of the boundary of the domain $\Gamma(t) = \partial\mathcal{O}_(t)$, and F is a functional of the domain $\mathcal{O}_(t)$ and the function $\vec{u}$. Typically, F is a nonlinear functional given by the derivatives of $\vec{u}$ on the boundary $\Gamma(t)$. Here the parameter λ represents various physical quantities that may change the behavior of the system.

Let us see how such problems arise in the growth of a solid tumor. Consider a (very much simplified) biological model of a tumor. In this simplified model, oxygen and glucose are considered "nutrient", with its density c satisfying $\delta c_t - \Delta c = -c$ for $x \in \mathcal{O}_(t)$. Since the rate of diffusion of nutrient is much faster than the rate of cell proliferation, it is also reasonable to take δ to be zero (Quasi-steady state approximation). The tumor grows with proliferation rate $= \mu(c - \tilde{c})$, where $\tilde{c}$ is a threshold concentration and μ is a parameter expressing the "intensity" of the proliferation (if $c > \tilde{c}$) or shrinkage by necrosis (if $c < \tilde{c}$) within the tumor. By the conservation of mass, proliferation rate $= \nabla \cdot \vec{v}$, where $\vec{v}$ is the velocity field within the tumor. If the tissue is assumed to be of porous medium type where Darcy's law (i.e., $\vec{v} = -\nabla\sigma$, where σ is the pressure) can be used (here the extracellular matrix is considered *"porous media"* in which the cell moves), then $-\Delta\sigma = \mu(c - \tilde{c})$, and the system is reduced to finding two unknown functions c and σ, together with the free boundary $\Gamma(t)$:

$$\begin{array}{ll} \delta c_t - \Delta c + c = 0, & x \in \mathcal{O}_(t), \\ c = \bar{c}, & x \in \Gamma(t), \\ -\Delta\sigma = \mu(c - \tilde{c}), & x \in \mathcal{O}_(t), \\ \sigma = \gamma\kappa, & x \in \Gamma(t), \\ V_n(t) = -\frac{\partial\sigma}{\partial n}, & x \in \Gamma(t), \end{array} \tag{14}$$

where $\bar{c}$ represents the concentration of the nutrient surrounding the tumor.

Models such as that above are mathematically extremely difficult. For example, if we set μ to be zero, then this problem reduces to the classical Hele-Shaw problem with surface tension (with many works devoted to it in the literature – searching Hele-Shaw on the title alone on MathSciNet returns 390 entries). Naturally, the tumor aggressiveness constant μ cannot be zero; thus this problem is more complex than the Hele-Shaw problem and the classical existence of a solution is in general not expected to be global in time. Fingering phenomenon is well observed for Hele-Shaw models. For our model, one of the most important questions is whether the tumor will spread out of control, or remains bounded. Since the study of the general classical existence (globally in time) becomes unrealistic (it is known that for Hele-Shaw with surface tension, global classical existence is not expected globally in time), it is natural to study the radially symmetric case as the first step. Although the tumor *in vivo* is unlikely to be radially symmetric, the tumor *in vitro* grown in a laboratory is likely to be of spherical shape. Thus the model does have implications in the application.

The study of this model started in the 1990's. In particular, if the tumor aggressiveness constant μ is large, or if the cell-to-cell adhesiveness constant γ is small, then the tumor is likely to spread. The radially symmetric case was studied in [15], where they established rigorously the global classical existence of a solution under natural biological assumptions; they also established the stability results: (i) there is a stationary solution under the natural biological data, (ii) for small μ, the stationary solution is asymptotically stable with respect to radially symmetric small perturbations. Note that this stability result is expected biologically since, as indicated above, μ describes the aggressiveness of the tumor.

It is natural to ask what happens to a non-radially symmetric solution. As mentioned above, the general study of non-radially symmetric solutions is difficult. Thus, as a first step, we like to start with a question that is simpler and yet important enough for the application: does a non-radially symmetric solution exist? This question is answered positively in [16], where they linearize the problem around a radially symmetric solution and then they formed an analytic series expansion near the free boundary. For the 2-space dimensional case, through a careful study using sharp PDE estimates, they proved that the series is convergent, and thus completing the proof of the existence of non-radially symmetric solution. The proof is limited to 2-space dimensional case since the PDE estimates are very lengthy and complex – they are of the type of the Cauchy-Kowalevski theorem. In [8], Hanzawa transformation is used to simplify the proof and extend the result to 3-space dimensional case.

In a recent series of papers [12, 13, 14] Friedman and Hu have developed bifurcation theories and stability theorems, combining Crandall-Rabinowitz theorem [5] with new estimates on the PDEs in addition to the fundamental PDE estimates [6, 17, 31]. The methods involve *very sharp estimates* on the solutions of PDEs, using dimension reduction by Laplace transform, and explicit expansion into series of spherical harmonics. They have considered the stationary solutions and proved, that given any $R > 0$, one can construct branches of stationary solutions with any number of fingers, that is, solutions with free boundary

$$r = R + \epsilon Y_{n,0}(\theta) + O(\epsilon^2), \quad n \geq 2, \qquad \mu = \mu_n(R) + \mu_{n,0}(R)\epsilon + O(\epsilon^2), \tag{15}$$

(here we assume $\gamma = 1$ for simplicity), for any small ϵ. In this model μ_j are monotone: $\mu_2(R) < \mu_3(R) < \mu_4(R) < \cdots$, for any $R > 0$. It is clear that the stability of the stationary solution is lost at the first bifurcation point $\mu = \mu_2(R)$. Friedman and Hu [12] actually established the stability result for the stationary solution for all $\mu < \mu_*(R)$ (here R is the radius of the stationary solution) and non-stability result for $\mu > \mu_*(R)$. Furthermore, they rigorously proved that $\mu_*(R) < \mu_2(R)$ for $R < \bar{R}$ and $\mu_*(R) = \mu_2(R)$ for $R \geq \bar{R}$, for some critical $\bar{R}$ which can be computed numerically in terms of the tumor aggressiveness constant

μ and the cell-to-cell adhesiveness constant γ. (It is also not surprising that the bifurcation result when γ is not normalized to 1 is given in terms of the ratio μ/γ.)

Of course, the bifurcation rigorously established in (15) describes only the behavior of stationary solution near the bifurcation point (i.e., $|\varepsilon|$ small). In reality, it is interesting to find out what happens for the bifurcation branch away from the bifurcation point, and this is where the numerical computation is needed: to find, by a homotopy method (a frequently used method in the classical study of PDEs), the steady state branches of solutions as the data moves away from the bifurcation point. The next task will be to find out the stability of these solutions, as this will give a strong hint as to whether the tumor will spread out of control.

While Darcy's law may be a good approximation for some solid tumors, for several models (ductal carcinoma in breast, brain tumor) the Stokes equation is more appropriate [9, 10, 11]. In this case the stress tensor is given by $\sigma_{ij} = -\sigma\delta_{ij} + 2\nu\Big(e_{ij} - \frac{1}{3}\bar{\Delta}\ \delta_{ij}\Big)$ where $\sigma = -\frac{1}{3}\sigma_{kk}$, $e_{ij} = \frac{1}{2}\Big(\frac{\partial v_i}{\partial x_j} + \frac{\partial v_j}{\partial x_i}\Big)$ is the strain tensor, $\bar{\Delta} = e_{kk} = \mathrm{div}\vec{v}$ is the dilation, and ν is the viscosity coefficient. If there are no body forces then $\dfrac{\partial \sigma_{ij}}{\partial x_j} = 0$, which can be written as the Stokes equation

$$-\nu\Delta\vec{v} + \nabla\sigma - \frac{1}{3}\nu\nabla\mathrm{div}\vec{v} = 0, \quad x \in \mathcal{O}_(t), \ \ t > 0. \tag{16}$$

Assuming that the strain tensor is continuous up to the boundary of the domain, we then obtain a boundary condition:

$$T\vec{n} = -\gamma\kappa\vec{n}, \quad x \in \Gamma(t), \ \ t > 0,$$

where T is the stress tensor: $T = \nu(\nabla\vec{v} + (\nabla\vec{v})^T) - (\sigma + \frac{2}{3}\nu\ \mathrm{div}\vec{v})I$ with components

$$T_{ij} = \nu\Big(\frac{\partial v_i}{\partial x_j} + \frac{\partial v_j}{\partial x_i}\Big) - \delta_{ij}\Big(p + \frac{2\nu}{3}\mathrm{div}\vec{v}\Big),$$

$\vec{n}$ is the outward normal, and κ is the mean curvature.

The free boundary condition is given by

$$V_n(t) = \vec{v}\cdot\vec{n}, \qquad x \in \Gamma(t). \tag{17}$$

Replacing, in the tumor model described above, Darcy's law by Stokes equation (16) while keeping the rest of the equations, we obtain a free boundary problem for a coupled system of Stokes equation and a diffusion equation.

The theoretical results established in [7, 12, 13] describe the behavior near the bifurcation point (i.e., $|\varepsilon|$ small). Again, it is interesting to find out what

happens for the bifurcation branch when the data moves away from the bifurcation point, and this is where the numerical computation comes in: to find, by the method of continuation, the steady state solutions as the data moves away from the bifurcation point, and to find out the stability of these solutions.

The theoretical study of the above tumor problems depends on the explicit formula of the radially symmetric solution and sharp PDE estimates. Explicit solutions will not always be available.

For example, let the tumor region be $\mathcal{O}_(t)$ and assume that there are several types of cells within the tumor: proliferating cells with density $p(x,t)$, quiescent cells with density $q(x,t)$. The nutrient density with the tumor is still denoted by $c(x,t)$. Proliferating cells change into quiescent cells at the rate $K_R(c)$, and they become necrotic at a rate $K_N(c)$. We use $K_B(c)$ to represents the balance between birth and death. Then, similar to Problem 1, the equations for conservation of mass are given by [33, 34]

$$\frac{\partial p}{\partial t} + \text{div}(p\vec{v}) = [K_B(c) - K_Q(c)]p + K_R(c)q, \qquad x \in \mathcal{O}_(t), \tag{18}$$

$$\frac{\partial q}{\partial t} + \text{div}(q\vec{v}) = K_Q(c)p - [K_R(c) + K_N(c)]q, \qquad x \in \mathcal{O}_(t), \tag{19}$$

where $\vec{v}$ is velocity of the cells within the tumor. This velocity is a result of the proliferation of cells and removal of necrotic cells. The nutrient $c(x,t)$ diffuses within the tumor and is therefore modeled by the diffusion equation, as before.

Consider the 2-space dimensional tumor. To handle the free boundary, we developed a moving grid that evolved with the boundary. Figure 1 shows the grid for a radially symmetric and a non-radially symmetric solution. Using a third order discretization scheme with $R = 2.5$, we computed the radially symmetric solution for a small random value of μ and then used parameter continuation implemented in Bertini to track this solution as μ varied.

Since the Jacobian matrix of the discretized polynomial system is rank deficient when evaluated at the radially symmetric solution corresponding to a (discretized) bifurcation value of μ, we monitored the condition number of the Jacobian matrix as we tracked along the branch of radially symmetric solutions. This process produced a clear indication of a potential (discretized) bifurcation value near $\mu = 3.7$ as shown in Figure 2. Further calculations, described below, indeed shows that this value corresponds to an approximation of $\mu_2(R)$.

To produce a better approximation of the bifurcation value near $\mu = 3.7$, we setup Bertini to take increasingly smaller steps along the radially symmetric solution branch near $\mu = 3.7$. The numerically computed value matches the theoretical value very well, where the two-dimensional theoretical bifurcation value was derived in the same way as the three-dimensional case. The three-dimensional

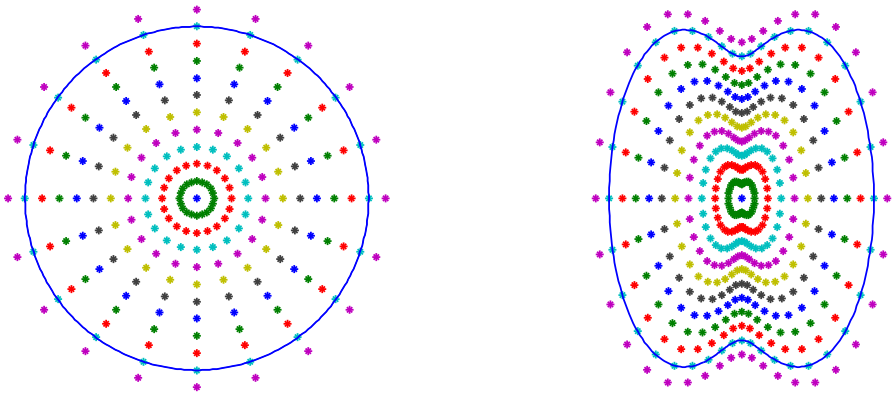

(a) Radially symmetric (b) Non-radially symmetric

Figure 1: Pictures of grids

case was rigorous derived and presented along with a three-dimensional theoretical bifurcation diagram in [12, 13, 14]. Table 1 compares these bifurcation values on a sequence of grids with the theoretical value $\mu_2(R) = 3.702687$. In this table, N_θ and N_R are the number of grid points in the angular and radial directions, respectively. It is clear that the numerical value converges to the theoretical value in our experiment.

N_θ	N_R	μ_2	abs. error
40	10	3.725819	0.023132
48	12	3.720450	0.017763
52	13	3.718400	0.015713
60	15	3.715204	0.012517
80	20	3.710412	0.007725

Table 1: Comparing (discretized) bifurcation value of μ_2 on a sequence of grids

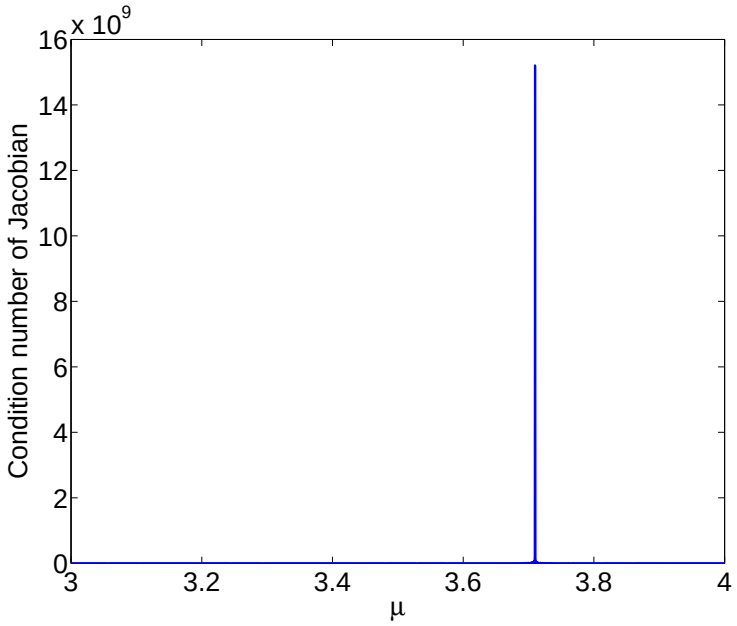

Figure 2: Condition number along radially symmetric solution branch as a function of μ

For these computations, the cost of numerically computing the radially symmetric solution is trivial compared with the cost of computing the condition number of the Jacobian matrix for the discretized system. All computations performed for this test are naturally parallelizable. For example, when using 200 processing cores, these computations with $N_\theta = 40$ and $N_R = 10$ took 3 minutes.

We verified the existence of a bifurcation branch by computing the tangent cone at these values. This produced two tangent directions which correspond to the radially symmetric branch and a symmetry-breaking branch. The numerically computed tangent direction for the symmetry-breaking branch compares favorably with its theoretical value, which was derived in the same way as the three-dimensional case discussed above. After computing the tangent direction of the symmetry-breaking branch, we forced Bertini to track along this branch. In Figure 3, we present two solutions computed by tracking in opposite directions on this non-radially symmetric branch. Since the initial steps along this symmetry-breaking branch are poorly conditioned, using high precision to perform this computation is crucial.

To further verify our numerical computations, we used our most coarse discretization ($N_\theta = 40$ and $N_R = 10$) to approximate the value of μ_4. The discretized

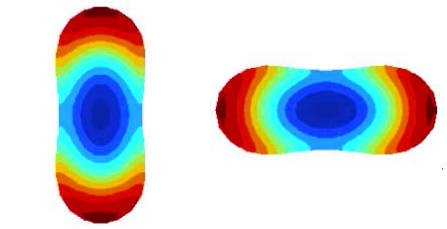

Figure 3: Non-radially symmetric solutions

value computed was 18.624 which compares favorably with the theoretical value $\mu_4(R) = 18.649$.

Though the solutions, for the two and three-dimensional model problems we investigated, became nonconvex, the domains remain star-shaped with respect to the origin and they never reached the point where we had to switch to a more sophisticated grid. We expect that this will be the case for more complicated systems and, as needed, will utilize adaptive grid generation.

Building from the success in the 2-space dimensional case, we performed calculations in the 3-space dimensional case. Using spherical polar coordinates and a discretization with $N_R = 20$, $N_\theta = 20$, and $N_\phi = 40$ grid points in the radial, inclination, and azimuth directions, respectively, we approximated $\mu_2(R)$ where $R = 2.5$ as above. The discretized value computed was 4.0398 which compares favorably with the theoretical value of $\mu_2(R) = 4.0422$.

As noted above, the theoretical description of the non-radially symmetric solution branches are known only locally near the bifurcation point, that is, when $|\varepsilon|$ is small. A numerical homotopy allows one to compute data about the non-radially symmetric solution branch far away from the bifurcation point.

Another problem dealt with was deciding whether a solution of the polynomial system is a solution of the differential equation. This was accomplished by sharpening the solution to a higher precision; interpolating to a finer grid; refining the interpolated solution to a solution within the desired tolerance for the polynomial system associated to the finer grid; and finally comparing the solutions on the different grids. Deciding whether a point is a solution of a polynomial system is a basic and nontrivial part of this procedure, which has been dealt with in Bertini by using multiple levels of precision.

Using adaptive-precision continuation methods, it is straightforward to check nonlinear stability directly. For example, given a solution of the time-independent three-dimensional system, we took a random perturbation and checked the development of the system with respect to time to numerically verify the stability results of [12, 13, 14].

References

[1] E.L. Allgower, D.J. Bates, A.J. Sommese, and C.W. Wampler. Solution of Polynomial systems derived from differential equations. Computing, 76 (2006), 1–10.

[2] E.L. Allgower and S.G. Cruceanu and S. Tavener. Application of numerical continuation to compute all solutions of semilinear elliptic equations. Advances in Geometry, 9 (2009), 371–400: available at `dx.doi.org/10.1515/ADVGEOM.2009.020`.

[3] E.L. Allgower and S.G. Cruceanu and S. Tavener. Turning points and bifurcations for homotopies of analytic maps. Contemp. Math., 496 (2009), 1–10: available at `dx.doi.org/10.1090/conm/496/09715`.

[4] D.J. Bates, J.D. Hauenstein, A.J Sommese, and C.W. Wampler. Bertini: software for numerical algebraic geometry. Available at `www.nd.edu/~sommese/bertini`.

[5] M.G. Crandall and L.H. Rabinowitz. Bifurcation from simple eigenvalues. J. Functional Analysis, 8 (1971), 321–340.

[6] A. Friedman. *Partial differential equations of parabolic type*. Princeton-Hall, Englewood Cliffs, New Jersey, 1964.

[7] A. Friedman. A free boundary problem for a coupled system of elliptic, hyperbolic, and Stokes equations modeling tumor growth. Interfaces and Free Bound., 8 (2006), 247–261.

[8] M. Fontelos and A. Friedman. Symmetry-breaking bifurcations of free boundary problems in three dimensions. Asymptotic Analysis, 35 (2003), 187–206.

[9] S.J.H. Franks, H.M. Byrne, J.P. King, J.C.E. Underwood, and C.E. Lewis. Modeling the early growth of ductal carcinoma in situ of the breast. J. Math. Biology, 47 (2003), 424–452.

[10] S.J.H. Franks, H.M. Byrne, J.P. King, J.C.E. Underwood, and C.E. Lewis. Modeling the growth of ductal carcinoma in situ. Mathematical Medicine & Biology, 20 (2003), 277–308.

[11] S.J.H. Franks, H.M. Byrne, J.C.E. Underwood, and C.E. Lewis. Biological inferences from a mathematical model of comedo ductal carcinoma in situ of the breast. J. Theoretical Biology, 232 (2005), 523–543.

[12] A. Friedman and B. Hu. Bifurcation from stability to instability for a free boundary problem arising in a tumor model. Arch. Rat. Mech. Anal., 180 (2006), 293–330.

[13] A. Friedman and B. Hu. Asymptotic stability for a free boundary problem arising in a tumor model. Journal of Differential Equations, 227 (2006), 598–639.

[14] A. Friedman and B. Hu. Stability and instability of Liapounov-Schmidt and Hopf bifurcation for a free boundary problem arising in a tumor model. Transactions of American mathematical society, 360 (2008), 5291-5342.

[15] A. Friedman and F. Reitich. Analysis of a mathematical model for growth of tumor. J. Math. Biology, 38 (1999), 262–284.

[16] A. Friedman and F. Reitich. Symmetry-breaking bifurcation of analytic solutions to free boundary problems: An application to a model of tumor growth. Trans. Amer. Math. Soc. 353 (2000), 1587–1634.

[17] D. Gilbarg and N.S. Trudinger. *Elliptic partial differential equations of second order*. Springer-Verlag, New York, New York, 1983.

[18] W. Hao, J.D. Hauenstein, B. Hu, Y. Liu, A.J. Sommese, and Y.-T. Zhang. Multiple stable steady states of a reaction-diffusion model on zebrafish dorsal-ventral patterning. Discrete and Continuous Dynamical Systems - Series S, 4 (2011), 1413–1428.

[19] W. Hao, J.D. Hauenstein, B. Hu, and A.J. Sommese. A three-dimensional steady-state tumor system. Applied Mathematics and Computation, 218 (2011), 2661–2669.

[20] W. Hao, J.D. Hauenstein, B. Hu, Y. Liu, A.J. Sommese, and Y.-T. Zhang. Bifurcation for a free boundary problem modeling the growth of a tumor with a necrotic core. Nonlinear Analysis Series B: Real World Applications, 13 (2012), 694–709: available at `doi:10.1016/j.nonrwa.2011.08.010`.

[21] W. Hao, J.D. Hauenstein, B. Hu, Y. Liu, A.J. Sommese, and Y.-T. Zhang. Continuation along bifurcation branches for a tumor model with a necrotic core. Journal of Scientific Computation, to appear.

[22] W. Hao, J.D. Hauenstein, B. Hu, T. McCoy, and A.J. Sommese. Computing steady-state solutions for a free boundary problem modeling tumor growth by Stokes equation. Journal of Computational and Applied

Mathematics, 237 (2013), 326–334: available online from Sept. 2012 at 10.1016/j.cam.2012.06.001.

[23] W. Hao, J.D. Hauenstein, B. Hu, and A.J. Sommese. A domain decomposition algorithm for computing multiple steady states of differential equations. Available at www.nd.edu/~sommese/preprints.

[24] W. Hao, B. Hu, and A.J. Sommese. Cell cycle control and bifurcation for a free boundary problem modeling tissue growth.

[25] W. Hao, G. Lin, Z. Xu, E. Rosen, A.J. Sommese, and M. Alber. Effect of Fitted Reaction Rates On Predicting Thrombin Production Using Blood Coagulation Model.

[26] W. Hao, J.D. Hauenstein, C.-W. Shu, A.J. Sommese, Z. Xu, Y.-T. Zhang. A homotopy method based on WENO schemes for solving steady state problems of hyperbolic conservation laws.

[27] J.D. Hauenstein and A.J. Sommese. Witness sets of projections. *Appl. Math. Comp.*, 217(7) (2010), pp. 3349–3354.

[28] J.D. Hauenstein, A.J. Sommese, and C.W. Wampler. Regeneration homotopies for solving systems of polynomials. *Math. Comp.*, 80 (2011), pp. 345–377.

[29] T.-L. Lee, T.Y. Li, and C.-H. Tsai. HOM4PS-2.0, Solving Polynomial Systems by the Polyhedral Homotopy Method. Software available at www.math.msu.edu/~li.

[30] T.-Y. Li. Numerical solution of polynomial systems by homotopy continuation methods. In *Handbook of numerical analysis*, Vol. XI. North-Holland Press (2003), Amsterdam, 209–304.

[31] G.M. Lieberman. *Second Order Parabolic Differential Equations*. World Scientific, Singapore, 1996.

[32] A.J. Lotka. Undamped oscillations derived from the laws of mass action. J. Amer. Chem. Soc. 42 (1920), 1595-1599.

[33] G.J. Pettet, C.P. Please, M.J. Tindall and D.L.S. McElwain. The migration of cells in multicell tumor spheroids. Bull. Math. Bio., 63 (2001), 231–257.

[34] B. Ribba, T. Colin and S. Schnell. A multiscale mathematical model of cancer, and its use in analyzing irradiation therapies. Theoretical Biology and Medical Modeling, 3 (2006), 1–19.

[35] A.J. Sommese and C.W. Wampler. *The Numerical Solution of Systems of Polynomials Arising in Engineering and Science*. World Scientific, Singapore, 2005.

[36] J. Verschelde. Algorithm 795: PHCpack: a general-purpose solver for polynomial systems by homotopy continuation. ACM Trans. Math. Software 25(2) (1999), 51–276. Software available at `www.math.uic.edu/~jan`.

[37] V. Volterra. Variazionie fluttuazioni del numero dindividui in specie animali convivent. Mem. Acad. Lincei., 2 (1926), 31–113.

[38] C.W. Wampler and A.J. Sommese. Numerical Algebraic Geometry and Algebraic Kinematics. Acta Numerica 20 (2011), 469–567.

[39] Y.-T. Zhang, A. Lander and Q. Nie, *Computational analysis of BMP gradients in dorsal-ventral patterning of the zebrafish embryo*, Journal of Theoretical Biology, **248** (2007), 579–589.